Solvent Effect on Reaction Barriers. The S_N2 Reaction. 1. Application to the Identity Exchange

Sason S. Shaik

Contribution from the Department of Chemistry, Ben-Gurion University of the Negev, Beer-Sheva 84120, Israel. *Received April 22, 1983*

Abstract: The valence-bond (VB) state correlation diagram model[1] is utilized to derive reactivity factors for S_N2 nucleophiles ($N:^-$) and substrates (RX) in various solvents. These reactivity factors are applied to analyze reactivity patterns in the ensemble of the identity reactions ($X^- + CH_3X \rightarrow XCH_3 + X^-$) and to bridge between gas-phase reactivity and reactivity in solutions. The trends in the reaction barriers are shown to arise from the interplay of intrinsic reactant properties and solvent properties in a manner which reflects *the nature of S_N2 as a transformation involving a single electron shift attended by bond interchange.*

A fundamental problem of any model which attempts conceptualization of chemical reactivity is its ability to handle solvent effects in a manner which can be integrated into a methodical thought process. We would like to suggest that the VB state correlation diagram model[1] can form a basis for such a conceptual framework.[2,3]

The S_N2 reaction poses an excellent target for applying the VB model. Since the pioneering work of the University College, London, school,[4] much decisive information has been learned about S_N2 through elegant mechanistic studies in solution[5] and in the gas phase.[6,7] Therefore, by its application to S_N2 reactions, the VB model meets the challenge of bridging between reactivity trends in the gas phase and in solution.

In this manuscript we lay the foundations. We derive reactivity factors and we apply them to the identity S_N2 reaction ($X^- + CH_3X \rightarrow XCH_3 + X^-$)[8] in order to show how the interplay of reactant properties and solvent properties generates the trends in the barrier's height. By that we hope to unravel some of the basis from which spring structure–solvent–reactivity relationships.[5]

I. S_N2 Reactivity Factors in Solution

The S_N2 reaction (eq 1) is a transformation that involves *synchronous* one-electron shift ($N: \rightarrow RX$) and bond interchange. This feature characterizes the electronic reshuffle experienced by

$$N:^- + R\text{–}X \rightarrow N\text{–}R + X:^- \qquad (1)$$

the "bare" reaction system and is invariant under change of the reaction medium. Therefore, the same state correlation diagram describes the chemical transformation in the gas phase[1b,c,g] and in solution.[9] Such a state correlation diagram in a solvent (s) is shown in Figure 1.

(1) (a) Shaik, S. S. *J. Am. Chem. Soc.* **1981**, *103*, 3692. (b) Shaik, S. S. *Nouv. J. Chim.* **1982**, *6*, 159. (c) Shaik, S. S.; Pross, A. *J. Am. Chem. Soc.* **1982**, *104*, 2708. (d) Shaik, S. S.; Pross, A. *Bull. Soc. Chim. Belg.* **1982**, *91*, 355. (e) Pross, A.; Shaik, S. S. *Acc. Chem. Res.* **1983**, *16*, 363. (f) Pross, A.; Shaik, S. S. *J. Am. Chem. Soc.* **1982**, *104*, 187. (g) Shaik, S. S. *Ibid.* **1983**, *105*, 4359; *Nouv. J. Chim.* **1983**, *7*, 201.

(2) For other discussions of solvent effects on reactivity of organic molecules using the VB method, see: (a) Warshel, A.; Weiss, R. M. *J. Am. Chem. Soc.* **1980**, *102*, 6218. (b) Warshel, A. *Acc. Chem. Res.* **1981**, *14*, 284. (c) Warshel, A. *Proc. Natl. Acad. Sci. U.S.A.* **1978**, *75*, 5250. (d) Warshel, A. *Biochemistry* **1981**, *20*, 3167. (e) Baughan, E. C.; Evans, M. G.; Polanyi, M. *Trans. Faraday Soc.* **1941**, *37*, 377. (f) Ogg, R. A., Jr.; Polanyi, M. *Ibid.* **1935**, *31*, 604. (g) A PMO method which includes solvent effect has been suggested by: Klopman, G. *J. Am. Chem. Soc.* **1968**, *90*, 223; Klopman, G.; Hudson, R. F. *Theor. Chim. Acta* **1967**, *8*, 165; Hudson, R. F. *Angew. Chem., Int. Ed. Engl.* **1973**, *12*, 36.

(3) A general theory of solvent effect for electron-transfer reactions has been described by: Marcus, R. A. *Annu. Rev. Phys. Chem.* **1964**, *15*, 155, and references therein. See also: Brunschwig, B. S.; Logan, J.; Newton, M. D.; Sutin, N. *J. Am. Chem. Soc.* **1980**, *102*, 5798. Sutin, N. *Acc. Chem. Res.* **1982**, *15*, 275.

(4) (a) De la Mare, P. D. B. *J. Chem. Soc.* **1955**, 3169. (b) Hughes, E. D.; Ingold, C. K.; Mackie, J. D. H. *Ibid.* **1955**, 3173. (c) Hughes, E. D.; Ingold, C. K.; Mackie, J. D. H. *Ibid.* **1955**, 3177. (d) De la Mare, P. D. B. *Ibid.* **1955**, 3180. (e) Fowden, L.; Hughes, E. D.; Ingold, C. K. *Ibid.* **1955**, 3187. (f) Fowden, L.; Hughes, E. D.; Ingold, C. K. *Ibid.* **1955**, 3193. (g) De la Mare, P. D. B. *Ibid.* **1955**, 3196. (h) De la Mare, P. D. B.; Fowden, L.; Hughes, E. D.; Ingold, C. K.; Mackie, J. D. H. *Ibid.* **1955**, 3200. (i) Pocker, Y. *Ibid.* **1959**, 3939.

(5) What follows is necessarily a partial list of contributions to the understanding of solvent effect on S_N2 reactivity: (a) Winstein, S.; Savedoff, L. G.; Smith, S.; Stevens, I. D. R.; Gall, J. S. *Tetrahedron Lett.* **1960**, *No. 9*, 24. (b) Swart, E. R.; LeRoux, L. J. *J. Chem. Soc.* **1956**, 2110. (c) Moelwyn-Hughes, E. A. *Trans. Faraday Soc.* **1949**, *45*, 167. (d) Bathgate, R. H.; Moelwyn-Hughes, E. A. *J. Chem. Soc.* **1959**, 2642. (e) Haberfield, P.; Nudelman, A.; Bloom, A.; Romm, R.; Ginsberg, H.; Steinherz, P. *Chem. Commun.* **1968**, *164*. (f) Haberfield, P.; Clayman, L.; Cooper, J. *J. Am. Chem. Soc.* **1969**, *91*, 787. (g) Haberfield, P. *Ibid.* **1971**, *93*, 2091. (h) Parker, A. J. *Chem. Rev.* **1969**, *69*, 1. (i) Cook, D.; Parker, A. J. *J. Chem. Soc. B* **1968**, 142. (j) Parker, A. J. *J. Chem. Soc.* **1961**, 1328. (k) Parker, A. J. *J. Chem. Soc. A* **1966**, 220. (l) Brodwell, F. G.; Hughes, D. L. *J. Org. Chem.* **1981**, *46*, 3571. (m) McLennan, D. J. *Aust. J. Chem.* **1978**, *31*, 1897. (n) Glew, D. N.; Moelwyn-Hughes, E. A. *Proc. R. Soc. London, Ser. A* **1952**, *211*, 254. (o) Parker, A. J. *Q. R., Chem. Soc.* **1962**, *16*, 163. (p) Johnson, M. D. *Annu. Rep. Prog. Chem.* **1962**, *58*, 171. (q) Bunnett, J. F. *Annu. Rev. Phys. Chem.* **1963**, *14*, 271. (r) Abraham, M. H. *Prog. Phys. Org. Chem.* **1974**, *11*, 1. (s) Abraham, M. H.; Abraham, R. J. *J. Chem. Soc., Perkin Trans. 2* **1975**, 1677. (t) Abraham, M. H.; Grellier, P. L. *Ibid.* **1976**, 1735. (u) Buncel, E.; Wilson, H. *J. Chem. Educ.* **1980**, *57*, 629; *Acc. Chem. Res.* **1979**, *12*, 42; *Adv. Phys. Org. Chem.* **1977**, *14*, 133.

(6) (a) Olmstead, W. N.; Brauman, J. I. *J. Am. Chem. Soc.* **1977**, *99*, 4220. (b) Payzant, J. D.; Tanaka, K.; Betowski, L. D.; Bohme, D. K. *Ibid.* **1976**, *98*, 894. (c) Smith, M. A.; Barkley, R. M.; Ellison, G. B. *Ibid.* **1980**, *102*, 6851. (d) Pellerite, M. J.; Brauman, J. I. *Ibid.* **1980**, *102*, 5993. (e) Lieder, C. A.; Brauman, J. I. *Ibid.* **1974**, *96*, 4028. (f) Brauman, J. I.; Olmstead, W. N.; Lieder, C. A. *Ibid.* **1974**, *96*, 4030. (g) Bohme, D. K.; Mackay, G. I. *Ibid.* **1981**, *103*, 978. (h) Bohme, D. K.; Young, L. B. *Ibid.* **1970**, *92*, 7354. (i) Tanaka, K.; Mackay, G. I.; Payzant, J. D.; Bohme, D. K. *Can. J. Chem.* **1976**, *54*, 1643. (j) Pellerite, M. J.; Brauman, J. I. *J. Am. Chem. Soc.* **1983**, *105*, 2672.

(7) Ab initio calculations are described by: (a) Kost, D.; Aviram, K. *Tetrahedron Lett.* **1982**, *23*, 4157. (b) Wolfe, S.; Mitchell, D. J.; Schlegel, H. B. *Can. J. Chem.* **1982**, *60*, 1291. (c) Baybutt, P. *Mol. Phys.* **1975**, *29*, 389. (d) Duke, A. J.; Bader, R. F. W. *Chem. Phys. Lett.* **1971**, *10*, 631. (e) Bader, R. F. W.; Duke, A. J.; Messer, R. R. *J. Am. Chem. Soc.* **1973**, *95*, 7715. (f) Dedieu, A.; Veillard, A. *Chem. Phys. Lett.* **1970**, *5*, 328. (g) Dedieu, A.; Veillard, A. *J. Am. Chem. Soc.* **1972**, *94*, 6730. (h) Keil, F.; Ahlrichs, R. *Ibid.* **1976**, *98*, 4787. (k) Anh, N. T.; Minot, C. *Ibid.* **1980**, *102*, 103. (l) Ishida, K.; Morokuma, K.; Komornicki, A. *J. Chem. Phys.* **1977**, *66*, 2153. (m) Wolfe, S.; Mitchell, D. J.; Schlegel, H. B. *J. Am. Chem. Soc.* **1981**, *103*, 7692. (n) Wolfe, S.; Mitchell, D. J.; Minot, C.; Eisenstein, O. *Tetrahedron Lett.* **1982**, *23*, 615. (o) Wolfe, S.; Mitchell, D. J.; Schlegel, H. B. *J. Am. Chem. Soc.* **1981**, *103*, 7694. (p) Morokuma, K. *Ibid.* **1982**, *104*, 3732.

(8) (a) Barriers in a variety of solvents were derived by: Albery, W. J.; Kreevoy, M. M. *Adv. Phys. Org. Chem.* **1978**, *16*, 87. (b) Experimental gas-phase barriers were derived by Brauman and Pellerite. See ref 6d, j. (c) Theoretical barriers were computed by Dedieu and Veillard (ref 7f) and Wolfe and co-workers (ref 7b, o).

(9) Our statement relates to the transformation of reactants to product. A change of mechanism ($S_N2 \rightarrow S_N1$) will also change the nature of the electronic reshuffle. One can easily show that such a change is unlikely for most CH_3X derivatives and one expects barriers of >60 kcal/mol for S_N1 reactions of these compounds. See, for example: Abraham, M. H.; McLennan, D. J. *J. Chem. Soc., Perkin Trans. 2* **1977**, 873. Abraham, M. H. *Ibid.* **1973**, 1893. The condition for an $S_N1 - S_N2$ competition is that $D_{R\text{–}X} + I_R - A_X - S_{R+} - S_{X\cdot}$ will not exceed ~20 kcal/mol which is a typical S_N2 barrier. $D_{R\text{–}X}$ is the bond energy, while S_{R+} and $S_{X\cdot}$ are the desolvation enegies of R^+ and $X:^-$. For a description of S_N1 see ref 1e and 2a. See also: Pross, A.; Shaik, S. S. *J. Am. Chem. Soc.* **1981**, *103*, 3702. Epiotis, N. D. "Theory of Organic Reactions"; Springer-Verlag: New York, 1978.

0002-7863/84/1506-1227$01.50/0 © 1984 American Chemical Society

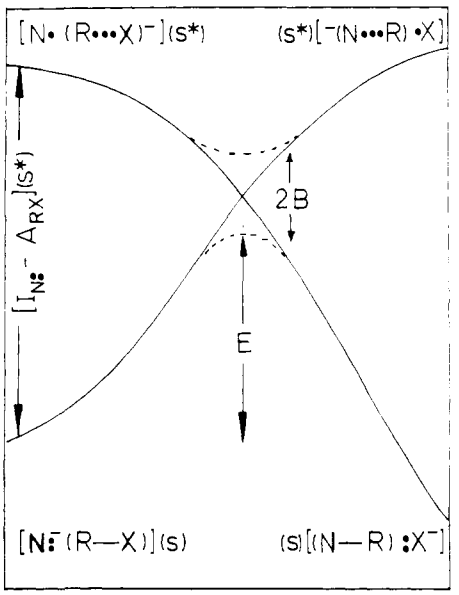

Figure 1. A valence-bond (VB) state correlation diagram for an S_N2 reaction in solution. The upper anchor states of the curves are obtained by a single electron transfer (e.g., $N:^- \rightarrow R-X$) from their corresponding ground states. The solvent configurations are common for the two curves. (s) indicates equilibrium solvation while (s*) indicates nonequilibrium solvation.

The reaction barrier (E) is a fraction (f) of the energy gap separating the intersecting curves at the reactant end, less the crossing avoidance (B), or quantitatively:

$$E = f[I_{N:} - A_{RX}](s^*) - B \qquad (2)$$

where $[I_{N:} - A_{RX}](s^*)$ is the vertical electron-transfer energy. The asterisk (s*) signifies that the species in the upper states, e.g., N· and $(R\cdots X)^-$, are under conditions of nonequilibrium solvation,[10] such that the solvent molecules surrounding them retain the original orientations they have around $N:^-$ and R–X.[11]

To estimate the vertical electron-transfer energies we employ thermochemical cycles similar to those that were used by Delahay[12] in his photoemission studies. The cycle in eq 3 sums as the vertical

$N:^-(s) \rightarrow N:^-(g)$	$\Delta E_1 = S_{N:}$	$(S > 0)$	(3a)
$N:^-(g) \rightarrow N\cdot(g) + e^-(g)$	$\Delta E_2 = I_{N:}(g)$	$(\equiv A_{N\cdot}(g))$	(3b)
$N\cdot(g) \rightarrow N\cdot(s)$	$\Delta E_3 = -S_{N\cdot}$		(3c)
$N\cdot(s) \rightarrow N\cdot(s^*)$	$\Delta E_4 = R[s^*,N:^-]$		(3d)
$N:^-(s) \rightarrow N\cdot(s^*) + e^-(g)$	$\Delta E = I_{N:}(s^*)$		(3e)

process $N:^-(s) \rightarrow N\cdot(s^*) + e^-(g)$, which describes ionization of $N:^-(s)$ under frozen solvent orientations. The vertical ionization potential, $I_{N:}(s^*)$, therefore reads:

$$I_{N:}(s^*) = I_{N:}(g) + S_{N:} - S_{N\cdot} + R[s^*,N:^-] \qquad (4)$$

$I_{N:}(g)$ is the *gas-phase* ionization potential (or $A_{N\cdot}$), while $S_{N:}$ and $S_{N\cdot}$ refer to *desolvation* energies of $N:^-$ and N·, respectively. $R[s^*,N:^-]$ in eq 3d describes the *reorganization energy* involved in changing the solvation shells from the equilibrium positions they assume around N·(s) to the original positions they had in $N:^-(s)$, thus generating N·(s*).

In a similar manner one obtains the energy change attending the process $R—X(s) + e^-(g) \rightarrow (R\cdots X)^-(s^*)$, and this is the required vertical electron affinity of the substrate, $A_{RX}(s^*)$, in solution:

$$A_{RX}(s^*) = A_{RX}(g) + S_{R\cdots X} - S_{RX} - R[s^*,(R\cdots X)^-] \qquad (5)$$

$S_{R\cdots X}$ is the *desolvation* energy of $(R\cdots X)^-$, while $R[s^*,(R\cdots X)^-]$ is the energy involved in reorganizing the solvent molecules from their equilibrium positions around $(R\cdots X)^-(s)$ to the original positions they had around R—X(s), and yielding $(R\cdots X)^-(s^*)$. Combining eq 4 and 5 one obtains the energy gap between the two curves in Figure 1.

$$[I_{N:} - A_{RX}](s^*) = [I_{N:} - A_{RX}](g) + S_{N:} - S_{R\cdots X} + S_{RX} - S_{N\cdot} + R[s^*,N:^-] + R[s^*,(R\cdots X)^-] \qquad (6)$$

Expressions for reorganization energies were derived by Marcus.[3,13] Using these expressions and the Born solvation model,[14] one can evaluate the reorganization energies (R) as fractions of the corresponding *desolvation* energies (S), as was done by Delahay.[12] The simple relationship is, of course, an approximation in all cases, but one expects it to pick up the physical essence of the problem. The relationship is shown in the equation:

$$R[s^*,N:^-]/S_{N:} = R[s^*,(R\cdots X)^-]/S_{R\cdots X} = (\epsilon - n^2)/[n^2(\epsilon - 1)]$$

$$(\epsilon - n^2)/[n^2(\epsilon - 1)] \equiv \rho \qquad (\rho < 1) \qquad (7)$$

ϵ is the static dielectric constant. n^2 is the optical dielectric constant that reflects the polarization response of the solvent to charges of the solute. Thus, the *reorganization energy* (R) is always some fraction (ρ) of the *desolvation energy* (S), and this fraction is a characteristic property of the solvent.[15] *ρ indicates the contribution of solvent reorganization to the reaction barrier in transformations, such as S_N2, which involve charge migration.* This meaning of ρ is projected from the expressions of the reactivity factors in eq 8–10 (obtained from eq 4–6):

$$I_{N:}(s^*) = I_{N:}(g) + S_{N:}(1 + \rho) - S_{N\cdot} \quad (S_{N\cdot} \approx 0) \qquad (8)$$

$$A_{RX}(s^*) = A_{RX}(g) + S_{R\cdots X}(1 - \rho) - S_{RX} \quad (S_{RX} \approx 0) \qquad (9)$$

$$[I_{N:} - A_{RX}](s^*) \approx [I_{N:} - A_{RX}](g) + S_{N:}(1 + \rho) - S_{R\cdots X}(1 - \rho) \qquad (10)$$

These equations reflect how the donor ability of the nucleophile, the acceptor ability of the substrate, and hence also the energy gap of the state correlation diagram are all determined by the interplay of an intrinsic reactant property (e.g., $I_{N:}(g)$), an intrinsic solvent property (ρ), and a solvent–reactant interaction property (e.g., $S_{N:}$).

To utilize the above relationships for estimating reaction barriers (eq 2), we still need to determine the reactivity factor (f) and to evaluate desolvation energies ($S_{R\cdots X}$) of radical anions. The full details are given as supplementary material (Appendix 1 there) deposited with this paper. What follow here (eq 13–17) are *simplified expressions* that faithfully reproduce the trends of the more elaborate expressions.

The radical anion $(R\cdots X)^-(s^*)$ obtains from the mixing of the VB forms $R\cdot :X^-$ and $R:^- \cdot X$ with weights (a^2) and (b^2) that reflect the relative stability of the configurations at their states of nonequilibrium solvation (s*), i.e.,

$$(R\cdots X)^-(s^*) = a^2[(R\cdot :X^-)(s^*)] \leftrightarrow b^2[(R:^- \cdot X)(s^*)] \qquad (11)$$

$$a^2 + b^2 = 1$$

The weights (a^2, b^2) depend on the energy separation, $\delta E(s^*)$, of the two VB configurations and on their interaction element β_{RX} ($\beta_{RX} \approx (D_{RR}D_{XX})^{1/2}$),[1b,c,g] such that

(10) $(R\cdot X)^-$ and $(R\cdot\cdot X)^-$ are the alternative ways we have used to describe the three-electron bond in the radical anion.[1b,c] The form appearing in the text is used for convenience.

(11) This is another way of saying that the solvent configurations are common for the two curves in accord with the Born–Oppenheimer approximation that holds for the reaction profile which arises from the avoided crossing of the two curves in Figure 1. For similar considerations see ref 2a and 3.

(12) Delahay, P. *Acc. Chem. Res.* **1982**, *15*, 40.

(13) Marcus, R. A. *Can. J. Chem.* **1959**, *37*, 155; *J. Chem. Phys.* **1956**, *24*, 966; *Discuss Faraday Soc.* **1960**, *29*, 21.

(14) For a detailed description of the Born model, see: Bockris, J. O'M.; Reddy, A. K. N. "Modern Electrochemistry"; Plenum Press: New York, 1970; Vol. 1, pp 49–179.

(15) Equation 7 is based only on electrostatic solvation (ref 14) and therefore one many envision that ρ will show also some dependence on the identity of the ion. The assumption of independence is necessary though if one wishes to construct a general scheme with a predictive ability.

$$b^2 = 0.5[1 - \Delta/(\Delta^2 + 4)^{1/2}];\ \Delta = \{\delta E(s^*)/(D_{RR}D_{XX})^{1/2}\} \quad (12)$$

$\delta E(s^*)$ reflects the relative gas-phase stability of $R:^-$ and $X:^-$ modified by differential solvation of the two VB configurations in nonequilibrium conditions (s*). The relative gas-phase (g) stability is given by the electron affinity difference $A_X.(g) - A_R.(g)$, while the differential solvation of the two VB figurations can be approximated as that of the corresponding anions, i.e.,

$$S_{R\cdot:X} - S_{R:\cdot X} \approx S_{X:} - S_{R:} \quad (S = \text{desolvation energies}) \quad (13)$$

Thus, $\delta E(s^*)$ becomes

$$\delta E(s^*) \approx A_X.(g) - A_R.(g) + (1 - \rho)[S_{X:} - S_{R:}] \quad (14)$$

$$\delta E(g) = A_X.(g) - A_R.(g)$$

The radical anion $(R\cdots X)^-$ is considered to have a more delocalized three-electron bond the greater its carbanionic contribution (b^2) (eq 11). In turn, *as the carbanionic contribution increases, the fraction (f) of the energy gap which enters the activation barrier (eq 2) also increases.*[1c,g] Thus, the effect of a solvent on the reactivity factor (f) can be predicted by using eq 12 and 14.

Having eq 12 and 14, the desolvation energy, $S_{R\cdots X}$, can be estimated as the sum of the desolvation energies of the two VB configurations weighted by their contributions (a^2) and (b^2). The desolvation energy of each configuration can be approximated by the desolvation energy of the corresponding anions, $X:^-$ and $R:^-$, and hence $S_{R\cdots X}$ will be given by:

$$S_{R\cdots X} \approx a^2 S_{X:} + b^2 S_{R:} \quad (15)$$

Therefore, the bond-acceptor ability of the substrate in eq 9 becomes

$$A_{RX}(s^*) \approx A_{RX}(g) + (1 - \rho)[a^2 S_{X:} + b^2 S_{R:}] \quad (16)$$

while the energy gap of the intersecting curves reads

$$[I_{N:} - A_{RX}](s^*) = [I_{N:} - A_{RX}](g) + (1 + \rho)S_{N:} - (1 - \rho)[b^2 S_{R:} + a^2 S_{X:}] \quad (17)$$

Using eq 8, 12, 14, 16, and 17 *one can now evaluate reactivity factors of S_N2 nucleophiles and substrates in the gas phase and in a variety of solvents.* Although these equations provide rough estimates, they contain the physical essence of the more elaborate expressions in the supplementary material, and as such they reproduce faithfully the trends of the detailed calculations. The compact number of variables promises that these equations can be integrated into a methodical thought process and provide *insight for making coherent predictions.*

Table I presents vertical ionization potentials for various S_N2 nucleophiles. It can be seen that each solvent[17,18] impairs the donor abilities of the nucleophiles,[19] and, in so doing, it also disturbs the order that is set by the intrinsic gas-phase property, $I_{N:}(g)$.

Table I. $I_{N:}(g)$ Values and $I_{N:}(s^*)$ Values in Water and DMF[a]

	$N:^-$	$I_{N:}(g)$[a]	$I_{N:}(H_2O^*)$[a]	$I_{N:}(DMF^*)$[c]	ΔG_t[c,d]
(1)	F^-	76	239.80	213.60	+12.0
(2)	Cl^-	83	203.12	188.10	+6.0
(3)	Br^-	78	185.64	175.10	+3.4
(4)	I^-	71	166.30	162.20	−0.5
(4a)	I^-			158.5–155.5	+(2–4)[d]
(5)	HO^-	44	210.92	184.60	+12.0
(5a)	HO^-		195[b]		
(6)	HS^-	53.5	176.70	161.50	+6.0
(7)	NC^-	89.5	200.26	189.55	+3.4

[a] All values in kcal/mol. $I_{N:}(s^*)$ follows from eq 8. $S_{N:}(H_2O) = 105, 77, 69, 61.1, 107, 79, 71$ for I^- to NC^- in respective order. The $S_{N:}$ values for F^-, Cl^-, Br^-, and I^- are Noyes' (ref 18d) dehydration energies (+2 kcal/mol) that reproduce $I_{N:}(H_2O^*)$ values of ref 12. Data source is discussed in the supplementary material (Appendix 5). $\rho(H_2O) = 0.56$; $\rho(DMF) = 0.48$ (ref 16). [b] This value is from ref 12. See ref 17d. [c] ΔG_t values (ref 18l) are used to calculate $I_{N:}(DMF^*)$; see ref 20a. $\Delta G_t = S_{N:}(H_2O) - S_{N:}(DMF)$. [d] See ref 20b.

The impairment of the donor abilities originates in the $(1 + \rho)S_{N:}$ term (eq 8) that accounts for the contributions of solvation and solvent reorganization to the ionization process.

Another trend is projected by comparing the $I_{N:}(s^*)$ values in the two solvents. Thus, the difference in the donor abilities of the same ion in H_2O and DMF is much larger than the corresponding free energies of the transfer ΔG_t (Table I, last column). The root cause is the $(1 + \rho)$ term (eq 8) that amplifies the differences in solvation. This amplification combined with the smaller reorganization factor, ρ, of DMF further accentuates the differences that originate in the ΔG_t values. Furthermore, even if ΔG_t is ~0, the vertical ionization potential will still be smaller in DMF than in H_2O owing to the smaller reorganization factor of DMF ($\rho = 0.48$ vs. 0.56; Table I, footnote *a*).[16] An example is provided by iodide in entry 4.

Let us turn to Table II to consider the acceptor abilities of substrates, and the degree of delocalization (b^2) of their radical anions (eq 11) in the gas phase (g) and in H_2O. The identity of the trends in the aqueous solution sets (II–IV) grants us some degree of confidence that the trends have a physical significance.

As expected, solvation of $(H_3C\cdots X)^-$ renders the H_3C–X substrates better electron acceptors relative to the gas phase. However, owing to the conditions of nonequilibrium solvation, the solvating power of the solvent takes only a partial expression as indicated by the $(1 - \rho)$ factor that multiplies the desolvation energies in eq 16. As a result, the acceptor abilities of the S_N2 substrates in H_2O retain the same order that is established in the gas phase (compare sets II–IV with set I). This gas-phase order is set by the C–X two-electron bond strength ($D_{R\text{-}X}$), the electron affinity of X ($A_X.$), and the three-electron bond energy $D_{R\cdots X}$, as shown in eq 18 that was extensively discussed before.[1c,g]

$$A_{RX}(g) = A_X.(g) - D_{R\text{-}X}(g) + D_{R\cdots X}(g) \quad (R = CH_3) \quad (18)$$

In addition to improving the acceptor ability of the substrate, the solvent also polarizes the three-electron bond. This can be understood by reference to eq 14 and 12, which together show that the solvent modulates the contribution (b^2) of the carbanionic VB form $(H_3C:^-\cdot X)$ in proportion to the differential solvation ($S_{X:} - S_{R:}$) of $X:^-$ and $H_3C:^-$. Thus $(H_3C\cdots F)^-$ and $(H_3C\cdots OH)^-$ become significantly less delocalized in H_2O relative to the gas phase because of the very strong solvation of F^- and HO^-.[17,18] For the rest of the anions this effect is much less significant since, in conditions of nonequilibrium solvation, the differential solvation ($S_{X:} - S_{R:}$ in eq 14) takes only partial expression $(1 - \rho)$. Consequently, the trends in the three-electron bond delocalization also remain similar to those in the gas phase. And one can distinguish between two groups: the radical anions of the methyl

(16) ϵ and n^2 values (at 298 K) are taken from "Handbook of Chemistry and Physics"; Weast, R. C., Ed.; The Chemical Rubber Co.: Cleveland, Ohio, 1972.

(17) $S_{HO:}$ values appear in: (a) Jorgensen, W. L.; Bigot, B.; Chandrasekhar, J. *J. Am. Chem. Soc.* **1982**, *104*, 4584. (b) Arshadi, M.; Kebarle, P. *J. Phys. Chem.* **1970**, *74*, 1483. (c) Gomer, R.; Tryson, G. *J. Chem. Phys.* **1977**, *66*, 4413. (d) Note that using the $S_{HO:}$ value in ref 17c and $\rho(H_2O) = 0.56$ one obtains $I_{HO:}(H_2O^*) = 190$ kcal/mol, very close to Delahay's result of ~195 kcal/mol.

(18) Different sources yield different values but identical trends; see: (a) Reference 17. (b) Arnett, E. M.; Johnston, D. F.; Small, L. E. *J. Am. Chem. Soc.* **1975**, *97*, 5598. (c) Arnett, E. M.; Small, L. E.; McIver, R. T., Jr.; Miller, J. S. *Ibid.* **1974**, *96*, 5638. (d) Noyes, R. M. *Ibid.* **1962**, *84*, 513; **1964**, *86*, 971. (e) Rosseinsky, D. R. *Chem. Rev.* **1965**, *65*, 467. (f) Reference 14. (g) Abraham, M. H., *J. Chem. Soc., Perkin Trans. 2*, **1973**, 1893. (h) Schuster, P.; Jakubetz, W.; Marius, W. *Top. Curr. Chem.* **1975**, *60*, 1. (i) Miller, J. *J. Am. Chem. Soc.* **1963**, *85*, 1628. (j) Reference 5m. (k) Abraham, M. H.; Liszi, J. *J. Inorg. Nucl. Chem.* **1981**, *43*, 143. (l) Abraham, M. H.; Liszi, J. *J. Chem. Soc., Faraday Trans. 1* **1978**, *74*, 1604.

(19) A similar conclusion was reached from HOMO energies of anions stabilized by small clusters of water: Anh, N. T.; Minot, C. *Tetrahedron Lett.* **1975**, 3905. HOMO energies correspond to the ionization energies at frozen geometries using Koopmans' theorem.

(20) (a) These ΔG_t are on the mole fraction scale. The differences rather than the absolute values are meaningful. (b) Using other sources, ΔG_t for, e.g., iodide is +(2–4) kcal/mol.

(21) Jortner, J.; Noyes, R. M. *J. Phys. Chem.* **1966**, *70*, 770.

Table II. C-X Bond Acceptor Abilities (A_{RX}) and Degrees of Three-Electron Bond Delocalization (b^2) for CH_3X Substrates[a]

		gas phase		H_2O				
		I[b]		II[c]		III[d]		IV[e]
	X	A_{RX}(g)	(b^2)	A_{RX}(s*)	(b^2)	A_{RX}(s*)	(b^2)	A_{RX}(s*)
(1)	F	−59	0.242	−11.1	0.204	−16.5	0.200	−36.0
(2)	Cl	−30	0.253	+4.8	0.242	+2.4	0.240	−12.2
(3)	Br	−21	0.246	+11.7	0.241	+8.8	0.241	−4.7
(4)	I	−10	0.240	+19.2	0.244	+17.1	0.243	+3.7
(5)	HO	−65	0.357	−18.5	0.307	−23.7	0.301	−42.0
(6)	HS	−41	0.340	−3.8	0.326	−8.4	0.322	−25.0
(7)	NC	−68	0.309	−34.4	0.304	−37.8	0.303	−52.7

[a] A_{RX} values are in kcal/mol. (b^2) is the weight of $R:^{\cdot}\cdot X$ (eq 11). [b] See ref 1c,g. [c] Results of the more accurate equations (28, 29, 35) in the supplementary material. Data source in Appendix 5 in the supplementary material. [d] Results of the approximate equations 12 and 16 of this text. $S_{H_3C:} = 63.5$ kcal/mol. [e] Results of equation 9. Desolvation energies of $(R\cdots X)^-$ are calculated independently using the Noyes-Jortner equation (ref 21). For details see Appendix 2 in the supplementary material.

Table III. C-X Bond Acceptor Abilities (A_{RX}) and Degrees of Three-Electron Bond Delocalization (b^2) for CH_3X Substrates in DMF and $PhNO_2$[a]

		H_2O[b]	DMF[c]		$PhNO_2$[c]	
		A_{RX}	A_{RX}	(b^2)	A_{RX}	(b^2)
(1)	F	−11.10	−10.63	0.209		
(2)	Cl	+4.80	+7.11	0.245	+9.66	0.247
(3)	Br	+11.70	+14.95	0.244	+16.00	0.245
(4)	I	+19.20	+24.10	0.242	+25.90	0.244
(5)	HO	−18.50	−17.18	0.313		
(6)	HS	−3.80	−2.70	0.328		
(7)	NC	−34.40	−31.39	0.306		

[a] A_{RX} in kcal/mol. Results of the more accurate equations (28, 29, 35) in the supplementary material. The approximate equations in the text (eq 12, 16) yield very close values (consult Table II). [b] Set II from Table II. [c] ρ(DMF) ≈ 0.48; ρ(Ph NO_2) ≈ 0.4; $\rho(H_2O) = 0.56$ (ref 16). Desolvation energies for X^-'s are estimated from ΔG_t data in ref 18k,l. $S_{H_3C:}$(DMF) = 64 kcal/mol; $S_{H_3C:}$(Ph NO_2) = 55 kcal/mol. Data source is discussed in Appendix 5 in the supplementary material.

halides (entries 1–4) which have quite localized three-electron bonds, and the group of $(H_3C\cdots OH)^-$, $(H_3C\cdots SH)^-$, and $(H_3C\cdots CN)^-$ which have more delocalized three-electron bonds. These trends have been obtained in all the sets of calculations which we tried, using desolvation energies from various sources with $S_{H_3C:}$ values ranging from 47–70 kcal/mol.

Table III shows the effect of DMF and $PhNO_2$ on the substrate acceptor ability, and on the degree of three-electron bond delocalization. The interesting feature arises when we compare the A_{RX} values in DMF and $PhNO_2$ with those in H_2O. Thus, despite the fact that solvation energies are larger in H_2O than in DMF or in $PhNO_2$, the latter two solvents stabilize the radical anions slightly better than does H_2O. This seeming contradication can be explained with the aid of eq 16. At the state of nonequilibrium solvation (s*) the radical anion $(H_3C\cdots X)^-$ *loses a fraction of its solvation energy in proportion to the reorganization factor* of the solvent, ρ. Therefore, the aprotic solvents $PhNO_2$ and DMF that have small reorganization factors will stabilize $(H_3C\cdots X)^-$(s*) better than, or as well as, does H_2O with the larger reorganization factor (footnote *c*, Table III). The same rule applies to other aprotic solvents that have a small ρ factor.

Having gained some insight into the properties of S_N2 nucleophiles and substrates, and into the effect of solvent reorganization, we can now analyze the barriers of the identity S_N2 transformation.

II. The S_N2 Identity Exchange ($X:^- + CH_3X \rightarrow XCH_3 + :X^-$)

Intrinsic barriers are becoming cornerstones in the epistemology of physical organic chemistry. This process can be witnessed by the recent important applications of the Marcus equation[3] to explain S_N2 reactivity trends.[8] At the same time, intrinsic barriers per se are perhaps among the least understood reactivity factors, and, rather than being considered as variables to be understood or explained, they are treated as means to predict other reactivity trends (in nonidentity reactions). Our aim in this section is to show that the trends in the intrinsic barriers arise from the interplay of reactant properties and solvent properties in a manner that reflects the nature of the S_N2 reaction as *a transformation involving simultaneous single electron shift and bond interchange*. In terms of our model this interplay is brought to the fore through the gap and the "slopes"[23] of the curves in the state correlation diagram (Figure 1).

The reactivity factors that determine the barrier height of identity reactions are ($I_{X:}$ - A_{RX}) and f (eq 2 and Figure 1). The gap factor ($I_{X:}$ - A_{RX}) is the donor–acceptor index of the reactant pair $(X:^-/CH_3X)$, and this index accounts for the *electron-shift aspect* of the transformation. The "slope" factor f *is the fraction of* the *energy gap that enters into the activation barrier*. This fraction is determined by the steepness of the curves under the characteristic distortions of the reaction coordinate.[23] As we have shown previously,[1c,g] f is proportional to the carbanionic character of the three-electron bond in the radical ion (b^2) (eq 11). Therefore, *variations* in (b^2) *set the value of* f and take into account the *bond-interchange* aspect of the transformations.[1c,g,23]

The interplay of these two aspects is likely to leave its mark on the reactivity patterns. According to eq 2 the ensemble of identity reactions will fall into families that share a common "slope" index, f. Within each such family the barriers are expected to vary as does the size of the donor–acceptor index ($I_{X:}$ - A_{RX}), with a sensitivity that is proportional to (b^2) through its proportionality to the "slope" index f.[23] Owing to this different sensitivities of the reaction families, the totality of the reactivity data is expected to exhibit donor–acceptor ($I_{X:}$ - A_{RX}) controlled patterns side by side with "slope" (b^2) controlled patterns.

Table IV presents reactivity factors and barriers of some identity reactions in the gas phase and in H_2O.[8] In accord with the predictions of eq 2, the reactions are seen to form two distinct families. The first family (entries 1–4) consists of the halide-exchange reactions for which the radical anions $(H_3C\cdots X)^-$ are quite localized (small b^2). And the second family (entries 5–7) involves exchange of X's which form more delocalized radical anions (larger b^2). The barriers within each group vary as does the size of ($I_{X:}$ − A_{RX}). Thus the best donor–acceptor X^-/CH_3X pair *within each group* has the smallest barrier, E (e.g., entry 4), while the worst donor–acceptor pair (e.g., entry 1) has the largest barrier (compare also entries 6 vs. 7).

The sensitivity of each family to the donor–acceptor index is seen to be proportional to the (b^2) index. In accord with the different sensitivities, the reactions barriers in the second family (entries 5–7) are seen to be larger than those of the first family

(22) Lewis, E. S.; Kukes, S. *J. Am. Chem. Soc.* **1979**, *101*, 417.

(23) The "slope" index f depends on the form of the curves as a function of the characteristic molecular distortions along the reaction coordinate (e.g., $f = 0.25$ for two parabolae; $f = 0.5$ for two straight lines having equal slopes, etc.). One can derive an expression that links b^2 to the steepness of descent of the two curves. For a given gap, the steepness of descent determines the value of f and this is the basis for eq 19. For discussions, see ref 1c, e, g.

Table IV. Reactivity Factors and Barriers (E) for $X^- + CH_3X \rightarrow XCH_3 + X^-$ in the Gas Phase and in H_2O[a]

		gas phase			H_2O			DMF
	X	$I_{X:} - A_{RX}$	(b^2)	E^b	$I_{X:} - A_{RX}$	(b^2)	E^d	$I_{X:} - A_{RX}$
(1)	F	135	0.242	26.2 (11.7)	250.9	0.204	31.8	224.2
(2)	Cl	113	0.253	10.2 (5.5)	198.3	0.242	26.5	180.9
(3)	Br	99	0.246	11.2 (-)	173.9	0.241	23.7	160.1
(4)	I	81	0.240	6.4	147.1	0.244	22.0	138.1
(5)	HO	109	0.357	26.6 (29.2)	213.4[c]	0.307	41.8	201.8
(6)	HS	94	0.340	24.2 (15.6)	180.5	0.326	$\geq$33.9[e]	164.2
(7)	NC	157	0.309	35.0 (43.8)	234.7	0.304	50.9	220.9

[a] $I_{X:}$ is taken from Table I ($I_{N:}$). A_{RX}, (b^2) are taken from sets I and II in Table II and from Table III (DMF). [b] Experimental barriers are from Brauman et al. (ref 6d,j). In parentheses are ab initio computed values from Wolfe et al. (ref 7o). E for I^-/CH_3I is estimated by us (ref 1c). [c] Using $I_{HO:}$ from Table I (entry 5a). [d] $\Delta G^{\ddagger}$'s from Albery and Kreevoy (ref 8a). [e] $\Delta G^{\ddagger}$ estimated from Lewis and Kukes (ref 22).

Table V. Calculated and Experimental Barriers (E)[a] for $X^- + CH_3X \rightarrow XCH_3 + X^-$

		H_2O			DMF		
		I[b]	II[d]				
	X	E(calcd)	E(calcd)	E(exptl)[e]	E(calcd)[f]	E(exptl)[e]	ΔE(calcd)[g]
(1)	F	37.18 (38.70)	34.43	31.8	32.86 (34.41)		4.32
(2)	Cl	33.98 (33.42)	31.14	26.5	30.32 (29.80)	22.71	3.66
(3)	Br	27.92 (28.61)	25.62	23.7	25.06 (25.70)	18.40	2.86
(4)	I	21.89 (23.39)	20.18	22	19.42 (20.81)	16.01	2.47[h]
(4a)	I						(3.60)[h]
(5)	HO	51.50 (50.65)	51.71	41.8	49.16 (48.41)		2.34
(5a)	HO	56.50 (55.53)[c]					7.34[c]
(6)	HS	44.84 (44.12)	41.68	$\geq$33.9	39.86 (39.22)		4.98
(7)	NC	57.44 (56.40)	56.65	50.9	53.52 (52.72)		3.92

[a] In kcal/mol. E(calcd) from eq 21 with the $I_{X:} - A_{RX}$ values of Table IV. (b^2) values are taken from Table II (set II) and Table III. [b] In parentheses: values obtained using Cl^-/CH_3Cl as the reference reaction, such that $f = 0.25[b^2(H_3C\cdots X)(s^*)]/[b^2(H_3C\cdots Cl)(g)]$; $E(\text{calcd}) = f(I_{X:} - A_{RX}) - 14$. [c] Using $I_{HO:} = 211$ kcal/mol (entry 5, Table I). [d] Using $I_{X:} - A_{RX}$ for the encounter geometries (details are given in Appendix 3 in the supplementary material). f values are as in footnote b above. [e] See footnotes d and e in Table IV. [f] Values in parentheses obtained as described in footnote b above. [g] $\Delta E = E(H_2O) - E(DMF)$; using set I for $E(H_2O)$. [h] Entry 4 is obtained with $\Delta G_t = -0.5$ kcal/mol while entry 4a with $\Delta G_t = +(2\text{–}4)$ kcal/mol (see also Table I, footnote d).

(entries 1–4). Thus a "slope"-controlled reactivity pattern is generated by such comparisons. For example, the larger barrier for the HS^- exchange, in comparison with, e.g., the Cl^- exchange (entries 6 and 2), originates in the delocalized three-electron bond of $(H_3C\cdots SH)^-$. This delocalization impairs the slopes of descent of the curves, thereby letting a higher fraction (f) of the gap ($I_{HS:} - A_{CH_3SH}$) enter the activation barrier.[1c,g]

These reactivity patterns are common to the gas-phase and solution data that appear in Table IV. This is in accord with the fact that *the reactivity factors in the gas phase and in aqueous solutions exhibit approximately the same trends*. Thus while the solvent affects only slightly the (b^2) index, it increases considerably the $I_{X:} - A_{RX}$ factor, and therefore the main solvent effect is to increase the gap between the curves that generate the barrier (Figure 1). This is the root cause for the consistent increase of the reaction barrier in aqueous solution relative to the gas phase (see Table IV). This trend is common to H_2O, DMF (last column in Table IV), and to other solvents that we have tried, e.g., EtOH, Me_2CO, Me_2SO, $PhNO_2$, etc. Thus the collage of reactivity patterns, generated by the identity S_N2 reactions, is seen to arise from *solvent amplification* of intrinsic gas-phase trends that, by themselves, are established via the interplay of the electron shift and the bond-interchange aspects of the S_N2 transformation.[1c,g]

In order to amplify the above insight, let us couch the above considerations by a quantitative application of eq 2. Previously,[1c,g] we have established the proportionality of the "slope" factor f and the delocalization index (b^2), such that:[23]

$$f = kb^2 \qquad (k = \text{proportionality factor}) \tag{19}$$

To obtain a more explicit expression for f we need the exact forms of the intersecting curves in Figure 1. Since this is obviously impossible, we need a starting point to calibrate the f values. A good starting point is $f = 0.25$, which is the value obtained when the reaction profile is mimicked by the intersection of two parabolic curves,[23] as in the Marcus theory.[3] Using $f = 0.25$ for the *gas-phase* halide-exchange reactions, we obtain that $k \approx 1$ (eq 19), because $(b^2) \approx 0.25$ for all the gas-phase halide-exchange reactions (Table IV). Under this calibration ($k \approx 1$) eq 19 becomes:

$$f \approx b^2 \tag{20}$$

To unify the expressions for the gas-phase and solution barriers, we assume constancy of the avoided crossing parameter, B,[1c] and we set $B = 14$ kcal/mol, as used previously for gas-phase reactions.[1c] Under these simplifications the barrier (*in solution and/or in the gas phase*) takes the expression:

$$E(\text{kcal/mol}) = b^2[I_{X:} - A_{RX}] - 14 \tag{21}$$

Using this expression we have calculated intrinsic barriers in H_2O and in DMF. These results are exhibited in Table V along with other sets of calculations. The experimental barriers, E(exptl), in the table are the values derived (by Albery and Kreevoy[8a]) from the Marcus equation using experimental rate data of nonidentity reactions. The different sets of calculation exhibit identical trends, and, at the same time, they also reproduce fairly well *the trends* in the "Marcus-experimental" barriers. This performance is encouraging from the point of view of the simple model equation (eq 21). Thus, the physical essence of the problem seems to be captured by the model in terms of the interplay between the electron-shift and bond-interchange aspects of the S_N2 transformation.

Since solvent effects have mechanistic significance in physical organic chemistry,[5g,h,r] it is important to derive a simple expression that provides some insight into these effects that are summarized in Tables IV and V. Following eq 17 (note that $a^2 + b^2 = 1$ and $S_{N:} \equiv S_{X:}$), the shift in the energy gap factor relative to the gas phase is:

$$[I_{X:} - A_{RX}](s^*) - [I_{X:} - A_{RX}](g) = 2\rho S_{X:} + b^2(1 - \rho)(S_{X:} - S_{R:}) \tag{22}$$

Since the (b^2) values are only slightly affected by the solvent, we can utilize a common (b^2) value for the gas-phase and solution

barriers in eq 21 (or eq 20 with $k \approx 1$). The solvent shift of the barrier relative to the gas phase becomes then (s = in a solvent; g = in the gas phase):

$$E_s - E_g = 2\rho b^2 S_{X:} + b^4(1-\rho)[S_{X:} - S_{R\cdot}] \approx 2b^2\rho S_{X:} \quad (b^4 << 1) \quad (23)$$

Put in words: *any solvent will magnify the intrinsic barriers in proportion to the delocalization index (b^2) of the radical anion, to the desolvation energy of the anion X:⁻ ($S_{X:}$), and to the solvent reorganization factor (ρ).*

In accord with eq 23, the consistently smaller barriers in DMF relative to H_2O (Table V) arise from a combination of smaller desolvation energies ($S_{X:}$) in DMF, and the smaller reorganization factor (ρ) of this solvent. The smaller ρ of DMF signifies that the contribution of solvent reorganization to the reaction barrier will be generally smaller in this solvent relative to H_2O. Thus, even if an anion is slightly better solvated in DMF relative to H_2O, the exchange barrier can still be smaller in DMF. An example of this kind is given in Table V (see ΔE values, in the last column, for entry 4: $I^-/(CH_3I)$.

Equation 23 can be utilized to explore another interesting trend. The last column in Table V presents ΔE(calcd) values which account for the change in the barrier height upon solvent replacement ($H_2O \rightarrow$ DMF). It can be seen that reactions with delocalized radical anions (large b^2) exhibit a greater sensitivity to solvent replacement than reactions with localized radical anions (small b^2). For example, the ΔE value for HS^- exchange is larger than that for Cl^- exchange (entries 2 and 6) despite the same free energy of transfer, $\Delta G_t(H_2O \rightarrow DMF)$, of the two anions and their approximately equal desolvation energies (see Table I, last column and footnote *a*). The same trend applies to the exchange reactions of NC^- vs. Br^- (entries 3 and 7, Table V). This behavior is in accord with the prediction of eq 23 that the sensitivity of any reaction will be proportional to the (b^2) index through the "slope" factor f (eq 20, 21).

This last conclusion originates in the assumption that is inherent in the application of our model (Figure 1) that solvent reorganization follows the reactants' reorganization along the reaction coordinate. And as a result of this follow-up, the reorganization of the solvent responds to the electronic features of the reactants (b^2). While this conclusion may sometimes be faulty,[24] it is worthy of further exploration. Moreover, this conclusion is credited with our previous experience that substrates with delocalized radical anions (e.g., CH_3SR, CH_3CN) are generally more sensitive to any variation that pertains to their S_N2 reactivity.[1g]

It is appropriate at this point to comment on the relationship between our model and the commonly used models that rely on transition-state properties to conceptualize reactivity.[5e-k,r-u,6a,g] The seemingly two different approaches are essentially similar since they both spring from the solvent response to charge reorganization. In this sense one can use the results of eq 23 to discuss properties of the transition state. For example, the $E_s - E_g$ quantity in eq 23 is always positive. In terms of the transition-state concept this will mean that all of the $(XCH_3X)^-$ transition states are less strongly solvated than their corresponding ground states, X^-/CH_3X, in any solvent. This is exactly the conclusion that was first drawn in the important work of Olmstead and Brauman,[6a] and later found support by Bohme and Mackay[6g] in their elegant studies of S_N2 reactions using HO^- solvated by small water clusters. Similar correlations between the two approaches can be made using other results of this work. For example, the relative solvation of transition states in H_2O and DMF can be discussed along the same lines using eq 23 and the known free energies of transfer of the anions (ΔG_t in Table I).

Thus, while we are not enamored with the numerical results, it does seem that the qualitative and quantitative aspects of the model lead to a logical conceptualization of reactivity trends within the ensemble of identity S_N2 reactions ($X^- + CH_3X \rightarrow XCH_3 + X^-$). The predictions of the model (Tables IV and V) neatly fit with the observation in the literature that reactivity trends within this unique set respond to the leaving-group ability of X^- rather than to its nucleophilicity[6d,j,7o,8a,25] and that this general trend remains invariant under a solvent change.

III. Conclusions

We have attempted to show here that the VB state correlation diagram model[1] can provide a basis for conceptualization *of both solvent effects and intrinsic reactivity trends* in the S_N2 reaction (eq 2). Utilizing the Marcus theory of nonequilibrium polarization,[13] solvent effect can be treated in terms of a compact number of well-defined properties related to solvent (ρ) and to solvent–reactant interactions (e.g., $S_{X:}$). This simplification endows the state correlation diagram model with an ability to unify reactivity trends, in the gas phase and in solution, and to make verifiable predictions in a coherent manner.

The model has, of course, limitations which spring from any attempt to generalize in chemistry.[15,26] In addition, achieving some measure of generality required us to sacrifice the detailed microscopic information. Yet one must hope that attainment of some unification is worthy of the loss of details, and that some of the details can be retrieved by further refinement of the model.[26]

Acknowledgment. The author is indebted to Professor J. I. Brauman for communicating his experimental results (ref 6j) prior to publication, and to Dr. S. Efrima for helpful discussions. Special thanks are due to Mrs. Y. Ahuvia for the typing of this manuscript.

Registry No. F^-, 16984-48-8; Cl^-, 16887-00-6; Br^-, 24959-67-9; I^-, 20461-54-5; HO^-, 14280-30-9; HS^-, 15035-72-0; NC^-, 57-12-5; FCH_3, 593-53-3; $ClCH_3$, 74-87-3; $BrCH_3$, 74-83-9; ICH_3, 74-88-4; $HOCH_3$, 67-56-1; $HSCH_3$, 74-93-1; $NCCH_3$, 75-05-8.

Supplementary Material Available: Four appendices that describe calculations of $A_{RX}(s^*)$, b^2, $S_{R\cdot X}$ (using the Noyes–Jortner equation), and energy gaps for the encounter geometries and one appendix with data source for the $S_{N:}$, $A_{X\cdot}$, and D_{R-X} values used in the manuscript (11 pages). Ordering information is given on any current masthead page.

(24) Kurz, J. L.; Lee, J.; Rhodes, S. *J. Am. Chem. Soc.* **1981**, *103*, 7651.

(25) See also: Lewis, E. S.; Kukes, S.; Slater, C. D. *J. Am. Chem. Soc.* **1980**, *102*, 1619.

(26) As noted by a referee, Figure 1 is drawn in terms of activation energies (E) while the reaction rate is determined by activation free energies (G^*). For more comments on this problem and on reaction dynamics in solution, see the pioneering study: Warshel, A. *J. Phys. Chem.* **1982**, *86*, 2218.